JOURNAL OF CATALYSIS 135, 223–235 (1992)

Transient Diffusion, Desorption, and Reaction Studies of Cyclopropane and Propylene with NaX and Eu/NaX Zeolites

ANGELOS M. EFSTATHIOU,* STEVEN L. SUIB,*,†,[1] AND CARROLL O. BENNETT*

*Departments of *Chemical Engineering and †Chemistry, University of Connecticut, Storrs, Connecticut 06269-3060*

Received March 18, 1991; revised January 6, 1992

The exchange of Eu^{3+} for Na^+ cations into the sodalite cages of X zeolite ($Eu_{25}Na_{11}X$) leads selectively to the isomerization reaction of cyclopropane to propylene. The latter reaction is catalyzed by Brønsted acid sites with an apparent activation energy of 10.6 kcal/mol. Sorption measurements of cyclopropane and propylene with Eu/NaX and NaX zeolites at 40°C support the view that Na^+ cations might be considered as sites for sorption of these molecules. Force fields created by Eu_4O^{10+} present in Eu/NaX zeolite may affect sorption. On the other hand, Brønsted acid sites in Eu/NaX enhance sorption of cyclopropane and propylene at 40°C. Chemisorption of propylene on the Brønsted acid sites of Eu/NaX is reversible and may occur via a propylene carbenium cation intermediate. Small amounts of hexene are formed during this sorption. The amount of Brønsted acid sites in the present Eu/NaX is at least 0.6 mmol/g cat.

INTRODUCTION

Hydrogen diffusion and sorption experiments with various ion-exchanged X zeolites from our laboratory have shown that H_2 is encapsulated at 1 bar H_2 pressure in the sodalite cages of X zeolite (*1*). Part of the argument for this assignment was based on the change in the quantity of H_2 encapsulated as Na^+ ions were partially exchanged with Cs^+, Ni^{2+}, and Eu^{3+} ions. Since no H_2 was encapsulated in Eu/NaX, it was reasoned that the encapsulated H_2 for the other zeolites was concentrated in the sodalite cages of X zeolite. The bulky ion Eu_4O^{10+} (*1, 2*) could then hinder passage of H_2 through the six-membered oxygen window of the sodalite cage. Electrostatic fields created by Eu_4O^{10+} may have also influenced sorption of H_2 in sodalite cages.

Infrared (*3, 4*) NMR (*5*), electron (*6*), and UV-visible (*4*) spectroscopies have been used to study sorption of propylene and cyclopropane in Na–faujasite and other zeolites. These methods provided evidence that Na^+ cations can be considered as sites for sorption of cyclopropane and propylene. Another way to probe such sorption is to exchange Na^+ for an appropriate cation that would occupy a position in the zeolite cavities that would result in a decrease of the sorption uptake of cyclopropane and propylene. This effect might occur not because of screening or blocking effects but because of inaccessibility of the cation to the sorbing molecule.

The present work is a study of sorption and reaction processes of cyclopropane and propylene in NaX and Eu/NaX zeolites. Europium (III) exchange was chosen for these studies since the kinetic diameters of cyclopropane and propylene are greater than the free aperture of the six-membered oxygen ring of the sodalite cage of X zeolite where the Eu^{3+} ions are located. Various transient and temperature-programmed methods have been employed with on line mass spectrometry, similar to those already reported (*7*).

Results reported here suggest that Na^+ cations can be considered as sites for cyclo-

[1] To whom correspondence should be addressed.

0021-9517/92 $3.00

propane and propylene sorption in NaX zeolite. Brønsted acid sites generated after dehydration at 380°C of the ion-exchanged Eu/NaX zeolite affect sorption of cyclopropane and propylene in the latter zeolite. It is shown that, unlike NaX, Eu/NaX selectively catalyzes the isomerization reaction of cyclopropane to propylene, probably because of Brønsted acid sites. Similar catalytic behavior has been reported for other rare-earth ion-exchanged zeolites (*8*), but to our knowledge not for Eu/NaX.

EXPERIMENTAL

Catalyst. Linde NaX zeolite (600 mesh) was purchased from Alfa Ventron Corp. (Danvers, MA) and used without further purification. The crystal size was about 1.2 μm as determined by scanning electron microscopy. This material was ion-exchanged by stirring 1 g of zeolite for 18 h in a round-bottom flask with 100 ml of a 0.05 *M* solution of $Eu(NO_3)_3 \cdot 6H_2O$ salt purchased from Alfa Ventron. The sample was filtered, washed with distilled deionized water, and dried under vacuum as previously described (*1*). The approximate formula (*1*) of the exchanged zeolite is $Eu_{25}Na_{11}X \cdot 10.5\ H_2O$. The amount of water was determined by a TGA experiment of heating the hydrated europium-exchanged zeolite to 380°C until no further loss was observed (similar to dehydration procedures used throughout this work), followed by dehydration of this material to 900°C to determine the total water content that could possibly lead to Brønsted acid sites as a result of the initial dehydration that corresponds to 24.52 wt% Eu (hydrated). X-ray powder diffraction results for the ion-exchanged, calcined, and treated (after reaction studies) zeolite showed that the sample retained its crystallinity. Prior to transient reaction studies the sample was checked *in situ* for residual H_2O by mass spectrometry. The zeolite bed (52 mg, powder) was supported by fine stainless-steel screens and glass wool.

Reactor-flow system. A once-through stainless-steel microreactor (0.75 ml) was used in this study. Response experiments have shown that the reactor behaves as an ideal mixed-flow reactor (CSTR) (*9, 10*). The flow system was the same as that described in Ref. (*10*). All the lines and valves after the reactor (including the inlet capillary and ion source of the mass spectrometer) were heated to 150°C, excluding possible adsorption of cyclopropane and propylene. The pure time delay of cyclopropane and propylene response, bypassing the reactor from the switching valve to the detector, was measured as previously described (*7*).

Mass spectrometry. The high-resolution mass spectrometer (Nuclide 12-90-G), data acquisition, calibration, and integration of the mass spectrometer response have been described (*11*). The mass numbers (*m/e*) of 42, 41, and 18 were used for cyclopropane (c-C_3H_6), C_3H_6, and H_2O, respectively. The similar cracking patterns of c-C_3H_6 and C_3H_6 limited the accuracy of gas-phase analysis of the mixture of these components during transient reaction studies of c-C_3H_6 with Eu/NaX zeolite.

Gas chromatography. Product distributions of the isomerization reaction of c-C_3H_6 were measured by a GC (CARLE 311) with a 1.8 m × 2 mm stainless-steel column packed with Chromosorb 102 and an H_2 flow rate of about 25 ml/min. A flame ionization detector (FID) was used. A complete separation of c-C_3H_6 and C_3H_6 was achieved by programming the column at 8°C/min from 45 to 180°C. GC peaks were measured with a microcomputer at the rate of 5 points/s. Integration was performed using the trapezoidal rule. Known dilute mixtures of c-C_3H_6 and C_3H_6 were prepared for calibration purposes.

Infrared spectroscopy. For the IR spectroscopic studies, the samples were pressed into thin wafers of about 10 mg/cm^2. Dehydration of the wafer sample placed in a specially designed quartz cell was performed in a vacuum line (10^{-5} Torr) at 380°C for 12 h. After dehydration or adsorption of pyridine, the cell was transferred to the spectrometer and mounted there without any exposure to

air. The spectrometer used was a Galaxy Series Model 4020 FTIR. The spectra were recorded as percentage transmission and obtained at room temperature. Introduction of pyridine into the Eu/NaX and NaX samples was accomplished by adsorption at room temperature for 10 min in a vacuum line, followed by evacuation at 120°C for 1 h.

Gas mixtures. Transient diffusion and reaction studies of c-C_3H_6 and C_3H_6 at 1 bar total pressure were performed with dilute mixtures of 0.5 mol% (3.8 Torr) sorbate gas in three different carrier gases: H_2, He, and Ar. Cyclopropane and propylene were CP grade (Matheson Co.), and Ar, He, and H_2 were zero grade (Aero All-Gas Co). Less than 2 ppm of propylene was measured by gas chromatography in the 0.5 mol% c-C_3H_6 mixtures, and less than 5 ppm of C_3H_8 was measured in the 0.5 mol% C_3H_6 mixtures. Argon was used in the temperature-programmed desorption (TPD) studies. Purification of this gas has been described elsewhere (*10*). The flow rate of all gases used was 30 ml/min (ambient).

RESULTS

An overview of the types of experiments presented below is given here to aid the reader. Two major types of experiments, sorption and desorption, are performed in our transient studies. In sorption experiments dimensionless gas-phase responses of (typically) hydrocarbon gases are monitored by high-resolution mass spectrometry. The gas phase response (Z) varies from 0, before the experiment, to 1, at equilibrium. The x axis represents time in these isothermal experiments. Three different experiments (forcing, mixing, and transient responses) are measured. The forcing function is the response of the mass spectrometer in the absence of catalyst via a bypass of the reactor. The mixing curve is the response with a catalyst for a switch of gas stream between two inert gases. The transient response is performed by switching from an inert gas to the gas of interest, typically a hydrocarbon (cyclopropane or propylene here).

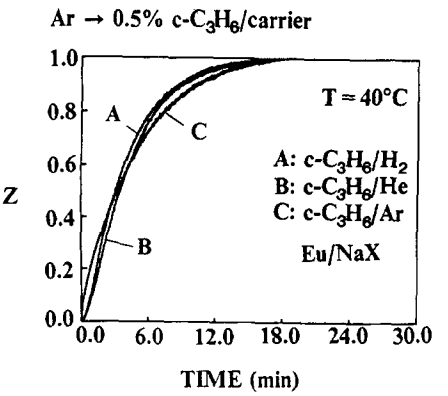

FIG. 1. Effect of carrier gas on the dimensionless gas-phase transient response of cyclopropane. Delivery sequence: Ar → c-C_3H_6/carrier. T = 40°C; carrier gas: H_2, He, and Ar; Eu/NaX sample used 52 mg.

An initial fast response for Z suggests that the gas-phase concentration of the gas of interest is high. An initial slow response for Z suggests that the gas-phase concentration is low and that the gas is sorbing on the catalyst. The difference between the mixing and transient response is the total amount of gas sorbed on the catalyst. The advantage of this particular method is that both the gas-phase response and the amount sorbed on the solid can be measured.

Desorption experiments are performed either isothermally or by temperature programming after initial sorption experiments by switching from the hydrocarbon feed to an inert gas and then heating.

(*A*) *Transient Sorption, Reaction, and Desorption of Cyclopropane in Eu/NaX*

Transient sorption data at 40°C for c-C_3H_6 in H_2, He, and Ar carrier gases with dehydrated Eu/NaX zeolite are given in Fig. 1. The dimensionless parameter Z represents the gas-phase concentration of c-C_3H_6 at some time t divided by the equilibrium gas-phase concentration (0.5 mol%, 3.8 Torr), reached after 18 min. The initial dZ/dt value for Ar carrier (curve C) is greater than that for either H_2 or He. However, between 6 and 18 min of sorption curve C lies below

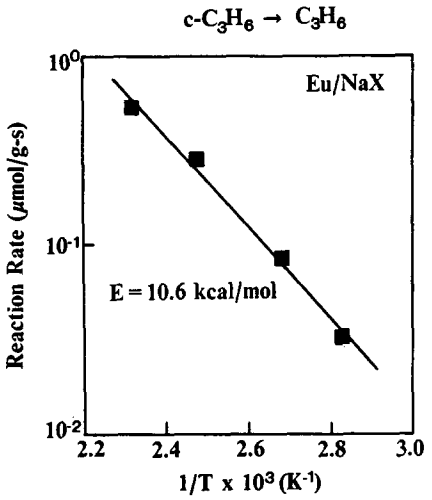

FIG. 2. Arrhenius plot for the cyclopropane isomerization reaction. $P_{c\text{-}C_3H_6}$ = 3.8 Torr; Eu/NaX sample used 52 mg; q = 30 ml/min (ambient).

those of H_2 or He. All three curves of Fig. 1 reach equilibrium (Z = 1) after 18 min. The equilibrium amount of c-C_3H_6 sorbed in Eu/NaX is 0.46 mmol/g independent of the carrier gas used.

On increasing the temperature of sorption between 80 and 160°C, the gas-phase c-C_3H_6 signal does not reach the equilibrium value of Z = 1 as in Fig. 1. Gas chromatographic analyses of the effluent stream reveal the presence of C_3H_6 in addition to that of c-C_3H_6. Results of this isomerization reaction are given in Fig. 2 after 20 min on c-C_3H_6/H_2 stream, at which time a pseudosteady-state is achieved. The corresponding reaction rates for C_3H_6 are 0.031, 0.083, 0.268, and 0.506 μmol/g-s for 80, 100, 130, and 160°C, respectively. The apparent value for the activation energy, E, of the c-C_3H_6 isomerization reaction is found to be 10.6 kcal/mol. Similar catalytic results are obtained for c-C_3H_6 in He or Ar carrier gases also.

Temperature-programmed desorption experiments for c-C_3H_6 sorbed at an equilibrium amount (0.46 mmol/g) at 40°C from H_2, He, and Ar carrier gas mixtures are given in Fig. 3. After sorption from 0.5 mol% c-C_3H_6/carrier mixture (Fig. 1; Z = 1), the feed is changed to Ar for 120 s at 40°C followed by a ramp of the temperature (TPD) in Ar flow. The mass spectrometer response at m/e = 42 and 41 shows two peak maxima (T_m) at 87 and 180°C in all cases. Gas chromatographic analyses indicate that at 87°C the c-C_3H_6 concentration is 2600 ppm and that of C_3H_6 is 50 ppm. At 180°C, no c-C_3H_6 but 440 ppm of C_3H_6 and 50 ppm of hexenes are found.

(B) Transient Sorption, Reaction, and Desorption of Propylene in NaX and Eu/NaX Zeolites

Transient sorption of C_3H_6 in Ar and He carrier gases with Eu/NaX at 40°C is shown in Fig. 4. The gas-phase transient response of C_3H_6 in He carrier is similar to that obtained for sorption of c-C_3H_6 in Eu/NaX (Fig. 1, curve B). However, due to chemisorption of C_3H_6 in Eu/NaX to be discussed later, the carrier gas effect is more pronounced for C_3H_6 in Ar (Fig. 4) than that for c-C_3H_6 in Ar (Fig. 1). Equilibrium gas-phase concentrations of C_3H_6 (Z = 1) at 40°C are obtained, corresponding to an amount sorbed of 0.62 mmol/g for either carrier. The transient response of C_3H_6 in H_2 carrier gas

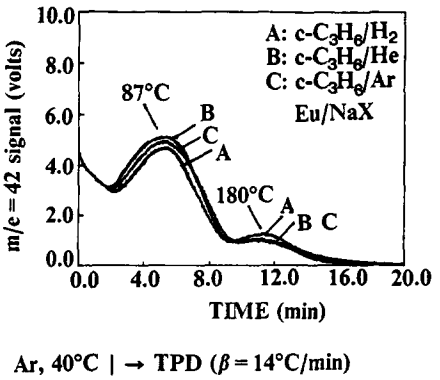

FIG. 3. TPD experiments based on m/e = 42. Experimental procedure: c-C_3H_6/carrier (40°C) until equilibrium is reached → Ar (180 s), 40°C → TPD (β = 14°C/min); carrier gas, H_2, He, and Ar; Eu/NaX sample used 52 mg.

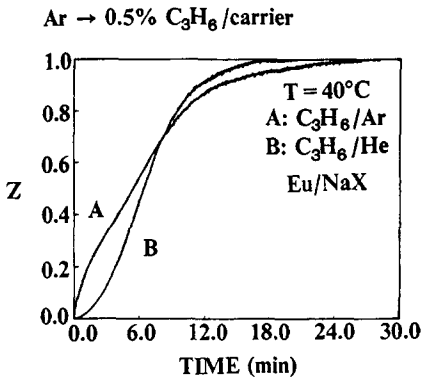

FIG. 4. Effect of carrier gas on the dimensionless gas-phase transient response of propylene. Delivery sequence: Ar → C_3H_6/carrier. T = 40°C; carrier gas, He, Ar; Eu/NaX sample used 52 mg.

is also very similar to that of C_3H_6 in He carrier gas.

Transient responses of C_3H_6 in He carrier gas with Eu/NaX and NaX zeolites at 130°C are shown in Fig. 5a. The response with Eu/NaX essentially reaches Z = 1 after 45 min on stream, whereas with NaX, Z = 1 is reached after 8 min on stream. Gas chromatographic analyses of the effluent stream of reactor during the 45 min on C_3H_6/He stream show the presence of hexenes in addition to that of propylene. Figure 5b gives the concentration of hexenes with time on C_3H_6/He stream. No hexenes were found during passage over NaX zeolite (Fig. 5a).

The amount of C_3H_6 consumed for either NaX or Eu/NaX in Fig. 5a is obtained from the difference in the area between the C_3H_6 gas-phase response and that of mixing (7). This is found to be 0.91 and 0.25 mmol/g for Eu/NaX and NaX, respectively. Integration of the response in Fig. 5b provides 0.18 mmol/g of hexenes after 45 min of reaction.

To further probe the results of Fig. 5, the following TPD experiment was performed. After reaction in C_3H_6/He at 130°C for 15 or 45 min on stream, the reactor is purged with Ar at 130°C for 10 min and then cooled to 80°C in Ar flow. During this treatment 0.08 and 0.20 mmol/g of C_3H_6 desorb after 15 and 45 min of reaction in C_3H_6/He, respectively. Then a TPD experiment is carried out. Figure 6 gives the results of this experiment. A significant increase in the amount of C_3H_6 desorbed from 0.21 to 0.40 mmol/g is measured on increasing the time on C_3H_6/He stream from 15 (curve A) to 45 (curve B) min. Desorptionof C_3H_6 in both cases occurs between 160 and 380°C. Less than 30 ppm of hexenes was measured by gas chromatography at 305°C for the results in Fig. 6.

A material balance is made to check the results of Figs. 5a, 5b, and 6. The amount of C_3H_6 consumed (hexene production) after a given time on C_3H_6/He stream is obtained

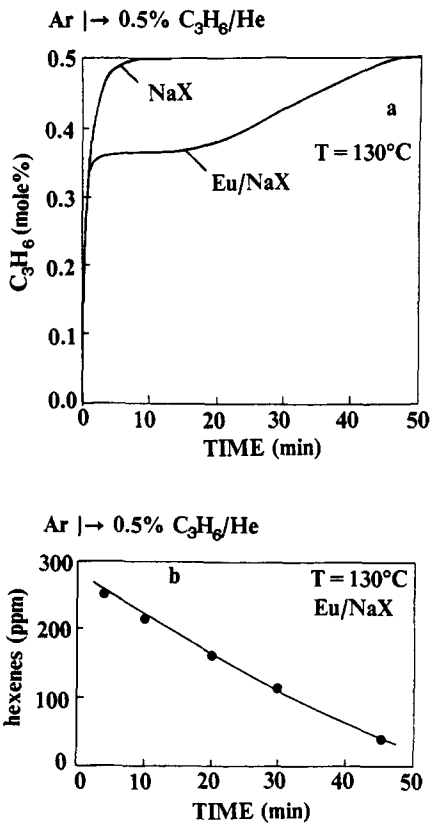

FIG. 5. (a) Dimensionless gas-phase transient reaction responses of propylene with NaX and Eu/NaX zeolites. Delivery sequence: Ar → C_3H_6/He (130°C); (b) gas-phase concentration of hexenes vs time for the delivery sequence in (a); NaX and Eu/NaX samples used 52 mg.

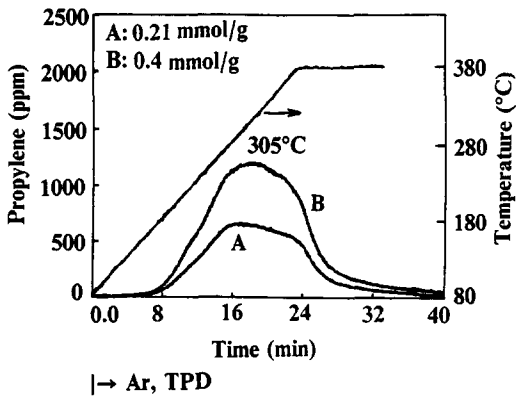

FIG. 6. Temperature-programmed decomposition reaction of the proposed propylene carbenium cation. Delivery sequence: C_3H_6/He(130°C, Δt) → Ar(130°C, 10 min) → cool to 80°C in Ar → TPD. (A) Δt = 15 min, (B) Δt = 45 min; Eu/NaX sample used 52 mg.

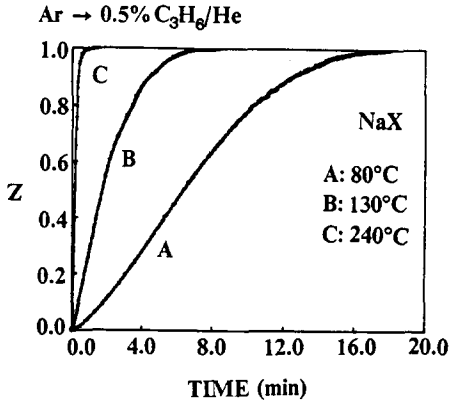

FIG. 7. Dimensionless gas-phase transient responses of propylene. Delivery sequence: Ar → C_3H_6/He (T); T = 80, 130, 240°C; NaX sample used 52 mg.

from the transient response in Fig. 5a as explained before, after correcting for the gas-phase C_3H_6 in the CSTR microreactor. This is found to be 0.41 and 0.91 mmol/g after 15 and 45 min on stream, respectively. This amount must agree with the sum of amounts of (a) C_3H_6 desorbed during the Ar purge (before the start of TPD in Fig. 6), (b) C_3H_6 obtained during the TPD of Fig. 6, and (c) hexenes produced during 15 min (0.085 mmol/g) or 45 min (0.18 mmol/g) on C_3H_6/He stream (Fig. 5b). A good agreement is obtained.

Transient responses for C_3H_6 sorption in NaX zeolite with He carrier gas at 80 and 240°C are shown in Fig. 7. For these sorption experiments equilibrium values for C_3H_6 are observed, 0.87 and 0.023 mmol/g for 80 and 240°C, respectively. The transient response of C_3H_6 at 130°C of Fig. 5a is also plotted in Fig. 7 on a different time scale. Results similar to those of Fig. 7 are obtained with H_2 carrier gas.

The equilibrium uptakes of C_3H_6 in NaX from a 3.8-Torr C_3H_6 pressure are plotted in Fig. 8 as millimoles per gram or molecules per unit cell vs temperature (isobar). Note the large decrease in the uptake of C_3H_6 as temperature is increased. The number of molecules of C_3H_6 sorbed per unit cell decreases from 25 at 40°C to less than 1 at 180°C.

Figure 9 gives the fit to a Langmuir isotherm for sorption results of Fig. 8 in the range 80–240°C at 3.8-Torr C_3H_6 pressure, as previously described (7). A value of −9.0 kcal/mol and −17.5 cal/mol-K are obtained for the enthalpy $\Delta H°$ and entropy $\Delta S°$ of sorption, respectively.

Temperature-programmed desorption experiments of C_3H_6 from Eu/NaX, after equilibrium sorption at 40°C from 0.5 mol% C_3H_6

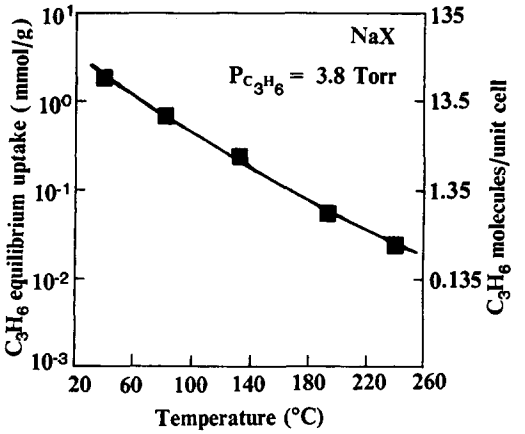

FIG. 8. Propylene equilibrium uptake (mmol/g, molecules/unit cell) vs temperature for NaX. $P_{C_3H_6}$ = 3.8 Torr.

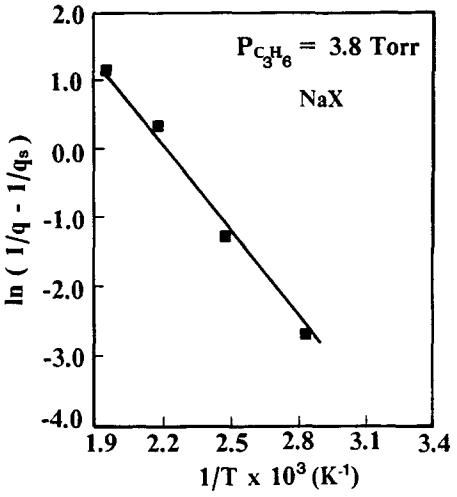

FIG. 9. Determination of limiting values for $\Delta H°$ (kcal/mol) and $\Delta S°$ (cal/mol-K) of sorption for propylene in NaX based on Langmuir isotherm.

in He and Ar carrier gases, are shown in Fig. 10A. After equilibrium is reached, the feed is changed to Ar for 10 min at 40°C followed by increase of the temperature at the rate of β = 14°C/min. Two peaks are observed for both carrier gases (T_m = 125 and 255°C). Corresponding TPD experiments with NaX zeolite are shown in Fig. 10B. In contrast to the results with Eu/NaX (Fig. 10A), only one peak (T_m = 125°C) is observed with NaX (Fig. 10B). The equilibrium amount of C_3H_6 sorbed in NaX at 40°C (Fig. 10B) is 1.55 mmol/g, and that in Eu/NaX (Fig. 10A) is 0.58 mmol/g. The latter amount is in good agreement with the sorption results of Fig. 4.

(C) *Acidity in Eu/NaX Studied by Infrared Spectroscopy*

Figure 11 shows the spectrum of chemisorbed pyridine in the form of pyridinium ion, which gives rise to the strong bands at 1541 and 1442 cm^{-1} and makes a major contribution to the band at 1490 cm^{-1}. The band at 1541 cm^{-1} is that of the Brønsted-bound form, and that at 1442 cm^{-1} is that of the Lewis-bound form. The infrared band at 1541 cm^{-1} after pyridine adsorption into NaX, pretreated in the same way as the Eu/NaX, was practically absent.

DISCUSSION

(A) *Brønsted Acid Sites in Eu/NaX Zeolite*

Many studies (*8, 12–14, 33*) presented evidence that for a rare-earth ion-exchanged zeolite the general reaction,

$$[RE(H_2O)_x]^{n+} \rightarrow [RE(OH)_x]^{(n-x)+} + xH^+ \quad (1)$$

occurs upon dehydration. The protons released form Brønsted acid sites in the zeolite, whereas the rare-earth cations migrate

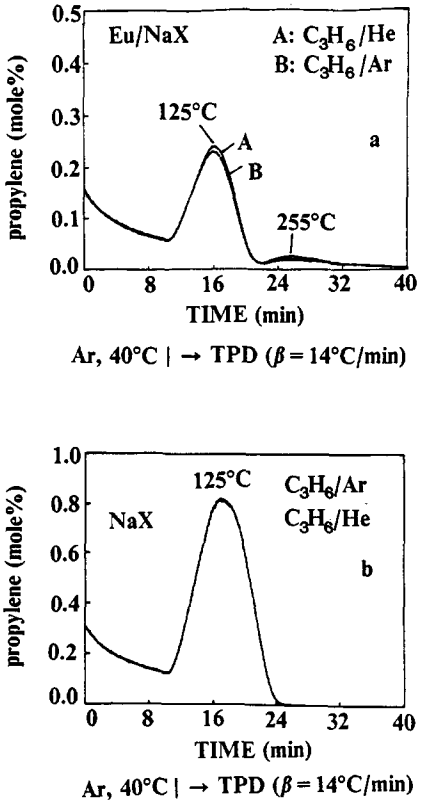

FIG. 10. TPD experiments of propylene with (A) Eu/NaX (52 mg) and (B) NaX (70 mg). Experimental procedure: Ar → C_3H_6/carrier (40°C) until equilibrium is reached → Ar (600 s), 40°C → TPD (β = 14°C/min).

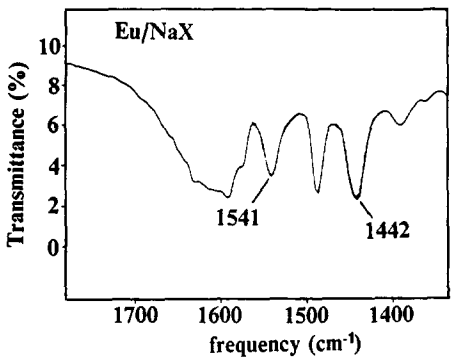

FIG. 11. Infrared spectrum of chemisorbed pyridine in Eu/NaX zeolite after dehydration at 380°C.

into the sodalite cage for X and Y zeolites forming a stable rare-earth oxide (*2, 12, 13*) according to

$$4[Eu(H_2O)_9]^{3+} \rightarrow Eu_4O^{10+} + 35H_2O + 2H^+. \quad (2)$$

The nonahydrate is implicated from luminescence lifetime measurements of hydrated EuNaX (*34*).

A detailed FTIR study on the hydrolysis of europium cations in zeolite X has recently appeared (*33*). An infrared OH stretching band at 3650 cm^{-1} (Si–OH) has been considered responsible for the formation of Brønsted acid sites in the $Na_{20}Eu_{17}X$ zeolite (*33*) due to hydrolysis of the initially hydrated Eu^{3+} cations. A similar band at 3668 cm^{-1} has been observed in the present work and by Bolton (*13*) for the La/NaY zeolite (infrared band at 3640 cm^{-1}). This infrared band is thought to arise from the protons released upon dehydration from the hydroxyl group attached to the rare-earth cation (*15*). Another distinct band at 3520 cm^{-1} has also been observed by Bolton (*13*) for La/NaY and has been assigned to the hydroxyl group attached to the rare-earth cation (*15*). This band has not been observed in the present zeolite perhaps because no $[Eu(OH)]^{2+}$ cation was present in the Eu/NaX after dehydration at 380°C. Relevant to this is our early proposal for the formation of Eu_4O^{10+} after dehydration at 380°C of the ion-exchanged prepared Eu/NaX zeolite (*1*).

For the purpose of this work the results of Fig. 11 are sufficient to provide evidence that the ion-exchanged prepared Eu/NaX zeolite after dehydration at 380°C leads to the formation of Brønsted acid sites (infrared band at 1541 cm^{-1}, (*16*)) capable of interacting with c-C_3H_6 and C_3H_6. Results of these interactions given in Figs. 1, 2, and 5 are discussed later. A more detailed infrared study on the effect of degree of Eu^{3+} ion exchange and other experimental conditions on the development of OH stretching and pyridine adsorption bands will be presented elsewhere (*17*).

(*B*) *Transient Diffusion and Sorption of Cyclopropane in Eu/NaX Zeolite*

Transient diffusion and sorption of c-C_3H_6 at 40°C depends on the carrier gas as shown in Fig. 1. Diffusion of c-C_3H_6 in Eu/NaX is initially faster for H_2 or He than Ar, although equilibrium values are independent of carrier gas. These phenomena have also been observed and discussed for diffusion of c-C_3H_6 in NaX zeolite (*7*). Collisional effects of c-C_3H_6 with the carrier gas inside the zeolite cavities and the walls rather than competition for sites of sorption were invoked to explain the aforementioned phenomena (*7*). Evidence that the transient uptake of c-C_3H_6 in NaX is only controlled by intracrystalline diffusion only has been given (*7*). This is also true for the results of Fig. 1, since mass transfer resistances outside the zeolite crystals were minimized (*7*).

The equilibrium amount of c-C_3H_6 sorbed at 40°C in Eu/NaX is 7.2 molec./u.c., and that in NaX is 21.9 molec./u.c. (*7*), after accounting for the difference in weight between Na^+ and Eu^{3+}. These results show that the amount of c-C_3H_6 sorbed in Eu/NaX is about one-third of that sorbed in NaX. If the force field created by Na^+ cations in NaX is responsible for c-C_3H_6 sorption as suggested (*3–6*), then the amount of c-C_3H_6 sorbed in NaX corresponds to the 3.2

Na^+/c-C_3H_6 molecule; this is based on the number of Na^+ cations accessible to c-C_3H_6 sorption (70 Na^+/u.c.) (*18*). In the absence of any other source that would contribute to c-C_3H_6 sorption in Eu/NaX, it is calculated that for the observed amount of c-C_3H_6 sorption in Eu/NaX 23 Na^+/u.c. are required. This number is twice the available one in the present Eu/NaX. Note also that the Na^+ cations inside the hexagonal prisms (16 Na^+/u.c.) (*18*) of NaX are the least likely to have been exchanged first. In addition, no c-C_3H_6 is expected to enter the hexagonal prisms of NaX (*18, 19*). Therefore, the large decrease observed in the amount of c-C_3H_6 sorbed in Eu/NaX (Fig. 1) compared to that in NaX (*7*) strongly suggests that Na^+ cations could be considered sites for sorption of c-C_3H_6.

The uptake of c-C_3H_6 by Eu/NaX at 40°C, which is two times greater than what might be expected, as mentioned in the previous paragraph, needs to be explained. Let us consider the ratio of the polarizing power (q/r) of Na^+ to that of Eu_4O^{10+} cation, the latter formed after exchange of Na^+ for Eu^{3+} in NaX followed by dehydration at 380°C (*1, 2, 12*). This ratio can be calculated based on the ionic radius (r) of 0.97 and 2.5 Å for Na^+ and Eu_4O^{10+}, respectively; the latter radius is that of a sphere inscribed in the Eu_4O^{10+} (Eu^{3+} is tetrahydrally coordinated with O^{2-} in the U site of the sodalite cage (*1, 2*)). This ratio is found to be 0.26. On the basis of a unit cell of X zeolite and after considering the composition of the present Eu/NaX zeolite, it is calculated that the polarizing power of Eu_4O^{10+} cations is one-third that of Na^+ cations, the latter being exchanged for an equivalent number of Eu^{3+}. Therefore, it seems that the effect of electrostatic force field created by Eu_4O^{10+} cannot be used to explain the higher sorption uptake of c-C_3H_6 in Eu/NaX than what might be expected based on the number of available Na^+ cations (sorption sites) in Eu/NaX compared to that in NaX.

The experimentally determined one-third ratio of equilibrium amount sorbed can also be calculated by assuming that the amount adsorbed is proportional to the product of the number of adsorption sites times q/r. If the 16 inaccessible sites in hexagonal prisms are excluded, then the ratio for Eu/NaX to NaX is

$$\text{ratio} = [(4.00)(6)]/[(1.031)(70)]. \quad (3)$$

This calculation suggests that some of the cyclopropane sorption may be due to sorption on sites other than the Brønsted sites, such as Na^+ or Eu^{3+} sites. This is an important point and we acknowledge a reviewer for this suggestion.

It is suggested that at 40°C chemisorption of c-C_3H_6 primarily occurs on the Brønsted acid sites of Eu/NaX (Fig. 11) via a cyclopropane carbenium cation (*8, 20*) without leading to an isomerization reaction. This is supported by the results of Figs. 1–3. In Fig. 1 no C_3H_6 is found, whereas in Figs. 2 and 3 at temperatures higher than 80°C the cyclopropane carbenium cation intermediate leads to C_3H_6 as a reaction product. Thus, this explanation is appropriate for interpreting the sorption results of c-C_3H_6 in Fig. 1, as discussed in the previous paragraphs. In fact, the interaction of c-C_3H_6 with Brønsted acid sites at room temperature has been shown for various zeolites having a different proton content (*4, 21, 22*). Considering the concentration of Eu^{3+} in the present Eu/NaX and the fact that the remaining Na^+ cations after exchange are likely to be found in the hexagonal prisms (*18*), where no sorption of c-C_3H_6 is expected, the uptake of c-C_3H_6 by Eu/NaX (Fig. 1) is mostly due to chemisorption on Brønsted acid sites. The exact nature of the species responsible for desorption from the first peak of the TPD of Fig. 3 is questionable. Isomerization occurs at temperatures as low as 80°C implying that at least some of the desorption from the first peak is due to Brønsted sites. Desorption from Na^+ and Eu^{3+} sites in this region is also possible.

The first peak appearing in the TPDs of Fig. 3 is similar to that obtained after c-C_3H_6 sorption in NaX for the same experimental

conditions (*7*). It is, therefore, likely that c-C_3H_6 desorbed from the Brønsted acid sites of Eu/NaX as discussed before has an interaction energy similar to that of c-C_3H_6 desorbed from the Na^+ cations.

The transient mass transport of c-C_3H_6 in Fig. 1 is affected by the concentration of Brønsted acid sites in Eu/NaX as well as the carrier gas as discussed before, but not significantly by the concentration of Na^+ cations. Simulations of the transients of Fig. 1 are expected to probe further these effects by providing kinetic information. This work is in progress.

(*C*) *Cyclopropane Isomerization in Eu/NaX Zeolite*

The isomerization reaction of cyclopropane to propylene has been widely used in the past as a test for the activity of acid-type solid catalysts including zeolites (*8, 23, 24*). The infrared results of Fig. 11 discussed before suggest that isomerization of c-C_3H_6 to propylene is catalyzed by the Brønsted acid sites in Eu/NaX, in line with catalytic studies on other acidic zeolites (*8, 20*). The results of Fig. 2 probe the large increase in the rate of isomerization of c-C_3H_6 with increasing temperature. The apparent activation energy for the isomerization reaction obtained here (10.6 kcal/mol) is smaller by 7 kcal/mol than that obtained with mordenites of different acidity (*21*). This activation energy was found to decrease with increasing Brønsted acidic strength (*21*). A study of the effect of Brønsted acidity in Eu/NaX (various Eu^{3+} loadings) on the kinetics of c-C_3H_6 isomerization reaction is in progress in our laboratory (*17*). Since isomerization of c-C_3H_6 (Fig. 2) has also been observed for He and Ar carrier gases, this suggests that the H_2 carrier gas does not promote other reactions (i.e., hydrogenation or hydrogenolysis).

The number of Brønsted acid sites in the present Eu/NaX can be calculated based on the information reporting (*12, 25*) that four rare-earth cations produce two acidic hydroxyl groups (see Eqs. (1) and (2)) and on the composition of Eu/NaX. This is found to be 0.8 mmol/g of zeolite. This number represents the maximum amount of Brønsted sites generated on dehydration of Eu^{3+} cations during dehydration. As mentioned in the Experimental section, it is possible that other Brønsted sites could be generated during dehydration of the zeolite; the amount of water in the formula for the dehydrated material in the Experimental section represents total water (including hydroxyl groups) remaining after dehydration at 380°C that is tightly bound. This information is discussed later based on the propylene desorption results of Fig. 6.

(*D*) *Transient Sorption, Reaction, and Desorption of Propylene in NaX and Eu/NaX Zeolites*

The transient sorption data of C_3H_6 in Fig. 7 show qualitative behavior similar to those of c-C_3H_6 sorption in NaX (*7*). However, for Eu/NaX in Figs. 1 and 4 the effect of carrier gas on the transient sorption is somewhat different for c-C_3H_6 than for C_3H_6; note the position of curve A with respect to that of curve B in Fig. 4, and similarly the position of curve C with respect to that of curve B in Fig. 1. It is suggested that (a) a different intracrystalline diffusivity value for c-C_3H_6 and C_3H_6 diffusion in Eu/NaX, and (b) different kinetics that describe diffusion and sorption of c-C_3H_6 and C_3H_6 in Eu/NaX are two main reasons that give rise to these results. The techniques applied here are appropriate to study these effects when a complete mathematical analysis of the transients of Figs. 1 and 4 is made. The latter is in progress.

The transient sorption and reaction data of C_3H_6 in Figs. 5a and 5b, and the TPDs in Figs. 6 and 10 show the interaction of C_3H_6 with the Brønsted acid sites in Eu/NaX. According to the literature (*4, 8, 26*) and the results of the present work the reaction scheme

$$C_3H_6 + H^+ \rightarrow C_3H_7^+ \rightarrow \text{dimerization to hexenes} \quad (4)$$

is suggested, where H^+ represents a Brønsted acid site in the Eu/NaX zeolite. The reversibility of the first reaction step in (4) is supported by the results of Fig. 6. That is to say, the amount sorbed during sorption experiments of Fig. 5 must match the amounts desorbed during desorption experiments of Fig. 6. Note that for H-ZSM5 zeolite, Kiricsi and Förster (*4*) suggested an irreversible step for the protonation of propylene. The fact that only hexenes have been produced via dimerization of propylene in the present Eu/NaX zeolite might lead to some conclusions about the mechanism of dimerization. It is suggested that a C_3H_6 molecule in the zeolite cavities reacts with a protonated propylene intermediate ($C_3H_7^+$) to give hexene and H^+. This proposed mechanism finds support in the work of Grady and Gorte (*27*) with H-ZSM5 zeolite.

The transient uptake of C_3H_6 with Eu/NaX in Fig. 5a can be discussed only qualitatively at this point. Comparing the transient response of C_3H_6 with NaX to that with Eu/NaX (Fig. 5a) it can be seen that the initial part of the transient response is the same for both zeolites. This may be because of the similar diffusion process in the two zeolites. Then as C_3H_6 builds up inside the zeolite crystal, it appears to interact with the Brønsted acid sites to form a propylene carbenium cation $C_3H_7^+$, followed by dimerization to hexene. The latter process appears to be an activated one based on the results of Figs. 4 and 5. The horizontal part of the transient in Fig. 5a for Eu/NaX seems to be the result of an accumulation of chemisorbed propylene on the Brønsted acid sites in agreement with the TPD results of Fig. 6.

The decrease in the concentration of hexenes with time on stream (Fig. 5b) is suggested to arise from steric hindrance and self-poisoning effects associated with hexenes, rather from the formation of inactive carbonaceous species (i.e., coke). Note that in the TPDs of Fig. 6 small quantities of hexenes were found, but no CH_4 was observed after H_2 treatment of the zeolite at the end of TPDs in Fig. 6. Thus during the TPD (with reaction) the process of Eq. (2) may be reversed with loss of Brønsted and Lewis sites as well as a decrease of formation of carbonaceous residue in the solid.

For the present Eu/NaX zeolite oligomerization of C_3H_6 occurred only to a small extent (Fig. 5b). On the other hand, for other acidic zeolites polymerization of C_3H_6 to a greater extent has been obtained (*4*, *8*, *27*). No propylene was found in the desorption experiment following adsorption of C_3H_6 on a H-ZSM5 zeolite (*27*), a result opposite to that found here (Fig. 6).

The amount of C_3H_6 desorbed from Eu/NaX during the 10-min isothermal Ar purge before the start of the TPD in Fig. 6 is found to increase with time on stream (compare the results after 15 and 45 min). On the other hand, the transient response of C_3H_6 with NaX in Fig. 5a indicates that equilibrium is achieved after 8 min. These results indicate that an accumulation of a less strongly chemisorbed propylene than that associated with the TPD peak of Fig. 6 occurs in the Eu/NaX zeolite. The TPD results of Fig. 10A, which suggest two kinds of chemisorbed propylene, are also relevant to this.

The TPD experiments related to the results of Fig. 6 provided 0.6 mmol of C_3H_6/g, this amount being associated with the Brønsted acid sites of Eu/NaX zeolite. This amount is consistent with the maximum amount (0.8 mmol/g) of Brønsted sites generated in the Eu/NaX zeolite as discussed before and the presence of Brønsted acid sites inaccessible to propylene sorption (*28*) as well as due to sorption on Lewis sites. In addition, the c-C_3H_6 sorption (0.46 mmol/g, Fig. 1) that occurred on the Brønsted acid sites is also a related result.

The TPD data of Fig. 3 can now be explained based on what has been mentioned in the previous paragraphs. The first peak (T_m = 87°C) is due to desorption of c-C_3H_6 from Lewis and Brønsted acid sites in Eu/NaX zeolite. As the temperature is increased above 80°C, c-C_3H_6 reacts with

Brønsted acid sites to give $C_3H_7^+$. This then decomposes at higher temperatures to give off propylene. Also, some of it reacts to give hexenes. The different T_m values obtained for the second peak in Figs. 3 and 10A are likely due to (a) effects of the initially sorbed C_3H_6 on the T_m value (*7, 29, 30*), (b) competitive reactions of c-C_3H_6 and C_3H_6 with the Brønsted acid sites, and (c) codiffusion effects of c-C_3H_6 and C_3H_6 for the case of Fig. 3, absent in Fig. 10A.

The equilibrium uptake of C_3H_6 at 3.8 Torr (isobar, Fig. 8) shows an exponential decrease as temperature is increased from 40 to 240°C. This behavior has also been observed for sorption of c-C_3H_6 in NaX (*7*) and NaY (*31*) zeolites. The heat of sorption for C_3H_6 obtained from the present work is in line with published calorimetric data (*19*). At 40°C (Fig. 8) a ratio of 5 Na^+/C_3H_6 molecule is obtained (based on 70 Na^+/u.c.), compared to 6 Na^+/C_3H_6 molecule reported for 5A and 13X zeolites (*5, 32*). The higher equilibrium uptake of C_3H_6 at 3.8 Torr in NaX (Fig. 10B) compared to that of c-C_3H_6 (*7*) could be explained by the stronger interaction between Na^+ and C_3H_6 than that between Na^+ and c-C_3H_6. This is due to the larger π-electron density of C_3H_6.

Finally, the large difference observed in the sorption amount of C_3H_6 at 40°C between Eu/NaX and NaX zeolites is evidence for Na^+ cations being sorption sites for C_3H_6 in NaX, as already discussed extensively for the case of c-C_3H_6.

The relatively long sorption times of Figs. 1, 4, 5, and 7 are not totally understood at present. Based on BET and pore size distribution measurements, the pores of NaX and Eu/NaX are not blocked. We are currently carrying out experimental and modeling studies to address this observation.

CONCLUSIONS

1. Cyclopropane sorbs on NaX at 40°C with a carrier gas effect. Sorption decreases at higher temperatures but there is no reaction, and sorbed cyclopropane is recovered unchanged by isothermal or temperature-programmed desorption (*7*).

2. Cyclopropane sorbs on Eu/NaX at 40°C to a lesser extent than on NaX, probably because the Na^+ cations in the supercages have been replaced by Eu_4O^{10+}. The latter cation is in the sodalite cages inaccessible to cyclopropane. However, Brønsted acid sites that are present on Eu/NaX but not on NaX result in a sorption higher than expected because of the decrease in Na^+.

At higher temperatures cyclopropane is isomerized to propylene over Eu/NaX. A little hexene is also formed.

3. Propylene sorbs to a much greater extent on Eu/NaX than on NaX. This may be due to sorption on Brønsted and Lewis sites. Hexenes are formed during this sorption, but the reaction is self-poisoning so that production of hexenes dies out as the amount of $C_3H_7^+$ reaches saturation.

4. TPD results show that most of the propylene sorbed on Eu/NaX is recovered as propylene according to the reversible process

$$C_3H_7^+ \rightarrow C_3H_6(g) + H^+.$$

A little hexene is also formed.

5. The shape of the uptake transients of cyclopropane and propylene in Eu/NaX shows carrier gas effects. The kinetics of diffusion and sorption of cyclopropane and propylene in Eu/NaX zeolite are also greatly affected by the concentration of Na^+ and Brønsted acid sites present in the zeolite.

ACKNOWLEDGMENTS

The support of the Department of Energy, Office of Basic Energy Sciences, Division of Chemical Sciences, and the help of Dr. Shen Y.-F. with the infrared analyses are gratefully acknowledged. We acknowledge Sang Sung Nam for TGA analyses.

REFERENCES

1. Efstathiou, A. M., Suib, S. L., and Bennett, C. O., *J. Catal.* **123,** 456 (1990).
2. Olson, D. H., Kokotailo, G. T., and Charnell, J. F., *J. Colloid Interface Sci.* **28**(2), 305 (1968).

3. Kiricsi, I., Tasi, G., Fejes, P., and Berger, F., *J. Mol. Catal.* **51,** 341 (1989).
4. Kiricsi, I., and Förster, H., *J. Chem. Soc., Faraday Trans. 1* **84**(2), 491 (1988).
5. Susic, M. V., Vucelic, D. R., Karaulic, D. B., and Pausak, S. V., *Surf. Sci.* **18,** 204 (1969).
6. Klier, K., *Adv. Chem. Ser.* **101,** 480 (1971).
7. Efstathiou, A. M., Suib, S. L., and Bennett, C. O., *J. Catal.* **135** (1992).
8. Jacobs, P. A., "Carboniogenic Activity of Zeolites," Ch. IV., Elsevier, Amsterdam, 1977, and references therein.
9. Efstathiou, A. M., and Bennett, C. O., *J. Catal.* **120,** 137 (1989).
10. Stockwell, D. M., Chung, J. S., and Bennett, C. O., *J. Catal.* **112,** 135 (1988).
11. Efstathiou, A. M., and Bennett, C. O., *J. Catal.* **120,** 118 (1989).
12. Moscou, L., and Lakeman, M., *J. Catal.* **16,** 173 (1970).
13. Bolton, A. P., *J. Catal.* **22,** 9 (1971).
14. Rabo, J. A., Angell, C. L., and Schomaker, V., *in* "Proceedings, 4th International Congress on Catalysis, Moscow, 1968" (B. A. Kazansky, Ed.). Adler, New York, 1968.
15. Rabo, J. A., Angell, C. L., Kasai, P. H., and Schomaker, V., *Disc. Faraday Soc.* **41,** 328 (1966).
16. Basila, Kantner, and Rhee, *J. Phys. Chem.* **68,** 3197 (1964).
17. Efstathiou, A. M., Simon, M., Borgstedt, E., Shen, Y.-F. and Suib, S. L., manuscript in preparation.
18. Breck, D. M., and Flanigen, E. M., "Synthesis and Properties of Zeolites L, X, and Y," Symp. Mol. Sieves, London, 1967.
19. Breck, D. W., *in* "Zeolite Molecular Sieves." Wiley, New York, 1974.
20. George, Z. M., and Habgood, H. W., *J. Phys. Chem.* **74,** 1502 (1970).
21. Förster, H., and Seebode, J., *in* "Proceedings, International Symposium on Zeol. Catal., Hungary, 1985."
22. Tam, N. T., Cooney, R. P., and Curthoys, G., *J. Catal.* **44,** 81 (1976).
23. Roberts, R. M., *J. Phys. Chem.* **63,** 1400 (1959).
24. Hall, W. K., Lutinski, F. E., and Gerberich, H. R., *J. Catal.* **3,** 512 (1964), and references therein.
25. Plank, C. J., *in* "Proceedings, 3rd International Congress on Catalysis, Amsterdam, 1964," Vol. 1, p. 727. Wiley, New York, 1965.
26. Förster, H., Seebode, J., Fejes, P., and Kiricsi, I., *J. Chem. Soc. Faraday Trans. 1* **83,** 1109 (1987).
27. Grady, M. C., and Gorte, R. J., *J. Phys. Chem.* **89,** 1305 (1985).
28. Moscou, L., *in* "Molecular Sieve Zeolites-H" (J. R. Katzer, Ed.), p. 337. Am. Chem. Soc., Washington, DC, 1977.
29. Choudhary, V. R., Srinivasan, K. R., and Akolekar, D. B., *Zeolites* **9,** 115 (1989).
30. Forni, L., Magni, E., Ortoleva, E., Monaci, R., and Solinas, V., *J. Catal.* **112,** 444 (1988).
31. Sajkowski, D. J., Lee, J. Y., Schwank, J., Tian, Y., and Goodwin, J. G., Jr., *J. Catal.* **97,** 549 (1986).
32. Barrer, R. M., Rees, L. V. C., and Shamsuzzoha, M., *Inorg. Nucl. Chem.* **28,** 629 (1966).
33. Bartlett, J. R., Cooney, R. P., and Kydd, R. A., *J. Catal.* **114,** 53 (1988).
34. Suib, S. L., Zerger, R. P., Stucky, G. D., Morrison, T. I., and Shenoy, G. K., *J. Chem. Phys.* **80,** 2203 (1984).